

RSC Advances



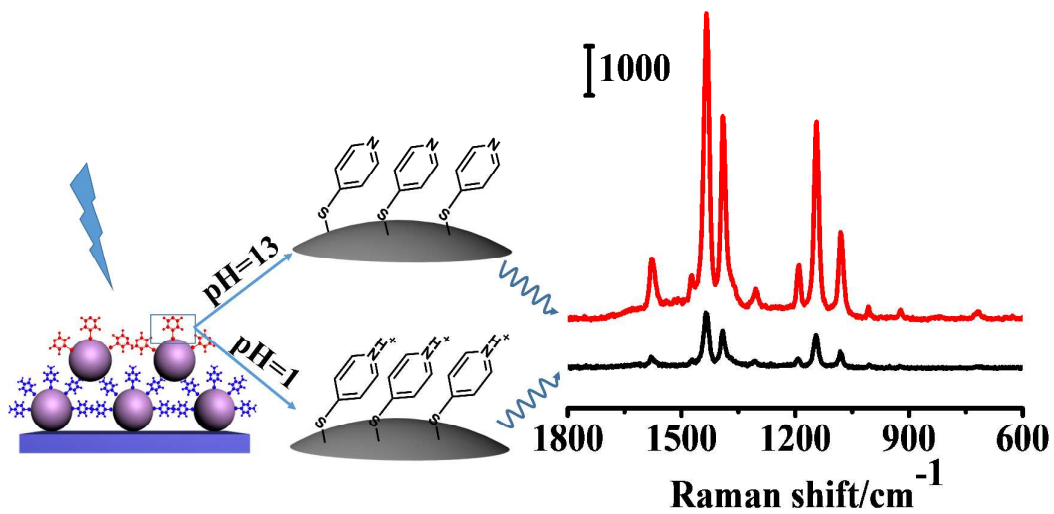
This is an *Accepted Manuscript*, which has been through the Royal Society of Chemistry peer review process and has been accepted for publication.

Accepted Manuscripts are published online shortly after acceptance, before technical editing, formatting and proof reading. Using this free service, authors can make their results available to the community, in citable form, before we publish the edited article. This *Accepted Manuscript* will be replaced by the edited, formatted and paginated article as soon as this is available.

You can find more information about *Accepted Manuscripts* in the [Information for Authors](#).

Please note that technical editing may introduce minor changes to the text and/or graphics, which may alter content. The journal's standard [Terms & Conditions](#) and the [Ethical guidelines](#) still apply. In no event shall the Royal Society of Chemistry be held responsible for any errors or omissions in this *Accepted Manuscript* or any consequences arising from the use of any information it contains.

Graphic Abstract



Effect of microenvironments on the properties of the molecular junctions can be elucidated by variation in surface-enhanced Raman scattering of 4-aminothiophenol interconnected in silver/4-aminothiophenol/silver junctions modified with different molecules.

ARTICLE

Effect of Adsorbed Molecules on Surface-enhanced Raman Scattering of Metal/molecule/metal Junctions

Cite this: DOI: 10.1039/x0xx00000x

Shuangshuang Li^{a,b}, Qun Zhou^{a,*}, Wenya Chu^a, Wei Zhao^a, Junwei Zheng^{a,b,*}

Received 00th January 2012,

Accepted 00th January 2012

DOI: 10.1039/x0xx00000x

www.rsc.org/

Metal nanoparticles assembled with functional molecules to form advanced structures has proven to have wide applications in molecular electronics and sensors. The microenvironments of the assemblies may largely influence the properties of the advanced structures. Herein, the silver/4-aminothiophenol/silver (Ag/PATP/Ag) structures are constructed to generate nanosized metal/molecule/metal junctions via layer-by-layer assembly technique. The effect of the microenvironments, such as adsorption of molecules on the junctions, on the properties of the molecular junctions is investigated by surface-enhanced Raman scattering of the PATP molecules interconnected in Ag/PATP/Ag junctions. It is demonstrated that the modification of molecules such as n-octanethiol, 1,8-octanedithiol, thiophenol 1,4-benzendithiol, and 4-mercaptopyridine, shows negligible effect on the enhanced electromagnetic field arising from the plasmon coupling of neighboring silver nanoparticles. The contributions from photoinduced charge transfer (CT) between the silver nanoparticles through the interconnected PATP molecules could be altered by the modification of the molecules. The large influence from the aromatic thiols is ascribed to the delocalization of the free electrons in the metal nanoparticles to the conjugated structure of the modified molecules.

Keywords: Molecular junction; Self-assembly; Silver nanoparticle; Charge transfer; Surface-enhanced Raman spectroscopy.

Introduction

Assembly of metallic nanoparticles into advanced structures with functional molecules through layer-by-layer assembly techniques has recently received increasing attention due to that metal nanoparticles, as the “building blocks”, are interconnected with molecules to spontaneously generate the junctions with gap size at nanometer or sub-nanometer level, which lead to the properties of the assemblies differing from those of individual nanoparticles.¹⁻³ A variety of interesting phenomena can occur on the metallic nanoparticle assemblies, with potential applications as optical antennas,⁴ nanolasers,⁵ single-molecule electronic devices,⁶ or single-molecule sensors.^{7, 8} It has been demonstrated that the coupling between the particles, orientation of the interconnected molecules, anchoring group of the molecules and environment of the junctions are the key factors to determine the properties of the junctions.⁹⁻¹² In this regard, the characterization of the molecular junction is essential to understand the properties of the molecular junctions. Surface-enhanced Raman scattering can provide useful information on the molecular junctions, because of its richness of spectral

information and high sensitivity and surface selectivity.¹³⁻¹⁵ For example, The SERS phenomena of metal nanoparticles have been mainly ascribed to two mechanisms: electromagnetic (EM) mechanism based on excitation of localized surface plasmon resonance of nanosized noble metals and chemical effect related to photo-induced charge transfer (CT) between energy levels of molecule and Fermi level of the metal. Importantly, as the metal nanoparticles approach to each other to generate a junction with a gap sized at nanometer or sub-nanometer level, plasmonic coupling between the nanoparticles can produce large electric field enhancement with SERS enhancement factors up to $\sim 10^{10}$ for a nanoparticle separation of 1 nm.¹⁶⁻¹⁸ On the other hand, enhancement factor from chemical effect for the junctions was estimated to be as large as 10^5 , which is more important than previously believed.¹⁹⁻²¹ Those contributions lead to huge overall SERS enhancement in the junction. In fact, during the past decade, SERS enhancements of 10^{14} - 10^{15} have been reported by many researchers for various molecules in the gap between metal nanoparticles, which enable SERS technique to be possibly used for single molecule detection.^{22, 23}

Nevertheless, little efforts have been devoted to investigate the effect of molecular environment on the properties of the metal/molecule/metal junction systems. In this paper, we fabricated silver/4-aminothiophenol/silver (Ag/PATP/Ag) junctions via layer-by-layer assembly technique. It was demonstrated that the SERS behaviors of the interconnected PATP molecules can be altered by the adsorption of various molecules that generated local molecular environment for the junctions. In particular, modification of molecules with a conjugated structure on the junctions may largely influence the photo-induced charge transfer between silver nanoparticles (AgNPs) through the interconnected PATP molecules, due to delocalization of free electrons in the nanoparticles to the conjugated structure of the modified molecules.

Experimental

Materials

4-Aminothiophenol (PATP), 4-mercaptobenzoic acid (4-MBA), thiophenol (TP) and n-octanethiol were obtained from Sigma-Aldrich; polyvinylpyridine (PVP) was purchased from Acros Organics. 1,4-Benzenedithiol (1,4-BDT), 4-mercaptopyridine (4-MPY), 1,8-octanedithiol were purchased from Tokyo Chemical Industry Co. Ltd. Silver oxide (Ag₂O) was purchased from Shanghai Chemical Reagent Company. The other chemicals were of analytical reagent grade and all the reagents were used as received.

Assembly of Ag/PATP/Ag Junctions

The silver colloid was prepared by the reduction of an Ag₂O saturated aqueous solution with hydrogen according to the literature protocols.²⁴ The average diameter of the particles was about 100 nm, estimated from the SEM image. The pH value of the resulting suspension was adjusted using diluted HCl and NaOH solutions in a 0.1 M NaCl aqueous solution.

The Ag/PATP/Ag junctions were prepared by the following layer-by-layer assembly procedure: Glass slides were first modified with PVP by immersing the slides into a PVP saturated ethanol solution for 24 h. After being thoroughly rinsed with ethanol and water, the slides were immersed to the silver colloid suspension for 12 h. A layer of the AgNPs was assembled on the surface of the slides. The adsorption of the PATP molecules on the assembled AgNPs was carried out by immersion of the glass slides assembled with the AgNPs in a 1 mM PATP ethanol solution for 6 h. Then the slides were washed with water and transferred into a silver colloid suspension for the assembly of the second layer of AgNPs. After that, the slide with double layers of AgNPs was immersed into a 1 mM 4-MBA, TP, 1,4-BDT, 4-MPY, n-octanethiol, or 1,8-octanedithiol ethanol solution for further modification.

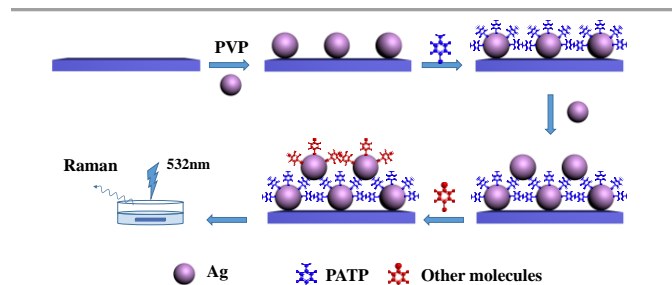


Fig.1 Schematic diagram of formation process of Ag/PATP/Ag junctions

Apparatus and Methods

The surface morphologies of the samples were measured on a Hitachi S4700 FE-SEM microscope. The UV-Vis spectra were measured on an Agilent Carry 60 UV-Vis spectrophotometer. The SERS spectrograms were measured on a RENISHAW Invia Raman microscope with the excitation wavelengths of 532 nm. The system employed a charge coupled device detector with a scanning time of 1 s and 50 × (NA 0.5) microscope objective to focus the laser beam onto a spot of ~2 μm². The Raman band of the silicon wafer at 520 cm⁻¹ was used to calibrate the spectrometer. All samples were measured in 0.5 cm deep solutions and the laser power is about 5mW.

Results and discussion

The assembly process of the Ag/PATP/Ag structure is shown in Fig. 1. In principle, the protonated pyridine groups of polyvinylpyridine (PVP) derivatized on a glass slide provide active sites for the adsorption of negatively charged AgNPs. Due to that there is electrostatic repulsion between the negatively charged AgNPs, it is expected that the assembly of AgNPs can only form a submonolayer of the nanoparticles on the substrate surface. Then, the bifunctional PATP molecules with thiol and amine groups at the opposite positions of the benzene ring are adsorbed on the surface of the assembled AgNPs. The PATP molecules may strongly interact with the AgNPs to form Ag-S bonds. On the other hand, the free amine group in PATP molecules can further interact with additional AgNPs. Consequently, a second layer of AgNPs can be formed spontaneously on the top of the first layer of AgNPs. Due to the PATP molecules exist as a monolayer on the surface of the first layer of AgNPs, the gap size in the Ag/PATP/Ag junctions would be at molecular size level.

The SEM images of the morphologies of the single and double assemblies of the AgNPs are shown in Fig. 2. As can be seen, the AgNPs were uniformly assembled into a submonolayer on the PVP-derivatized glass surface (Fig. 2A). Most of the particles existed separately as a result of the electrostatic repulsion between the particles. The adsorption of PATP molecules on the AgNPs had no obvious effect on the assembled structure of the AgNPs. The amine group at *para* position in the structure of the adsorbed PATP molecules is free and can interact with additional silver nanoparticles to form a second layer of the nanoparticles. The new layer of AgNPs can be clearly viewed as the AgNPs were assembled onto the PATP-modified AgNPs in the first layer (Fig.2B). Besides, some AgNPs were inserted into the first layer, resulting in a distinguishable increase in the density of the AgNPs in the first layer. This is because the modification of PATP molecules on the surface of the AgNPs in the first layer leads to vanishing of the original electrostatic repulsion between the AgNPs, then more AgNPs can be accommodated in the first layer. Nevertheless, it can be seen that most of the new coming AgNPs were also tightly attached to the original AgNPs in the first layer through the interaction with the amine groups of the PATP molecules adsorbed on the original AgNPs. Therefore, during the second layer assembly, the new coming AgNPs were mainly linked to the original AgNPs in the first layer to form the Ag/PATP/Ag junctions.

The extinction spectra of the silver colloid and assemblies of the silver nanoparticles were measured, the results are shown in Fig.2C. Two bands at 505 and 420 nm were observed for the

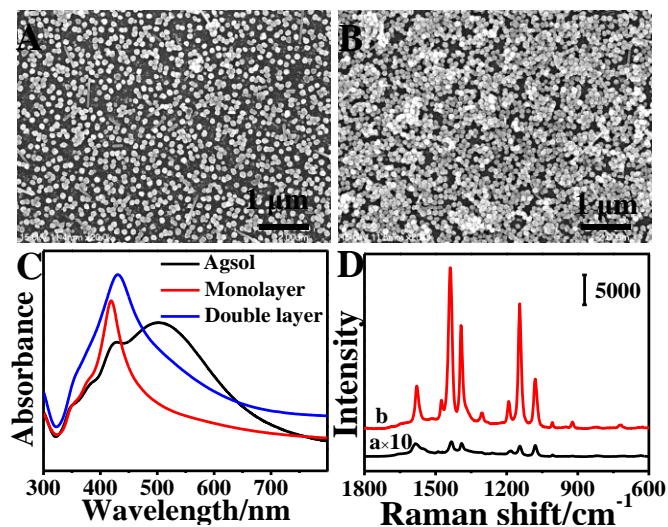


Fig. 2 SEM graphs of assemblies of single layer (A) and double layer (B) of AgNPs on PVP-modified glass, (C) extinction spectra of silver sol (black line), single layer (red line) and double layers (black line) of AgNPs on PVP-modified glass, (D) SERS spectra of PATP molecules adsorbed on single layer of AgNPs (black line) and interconnected in Ag/PATP/Ag junctions (red line).

silver colloid (black line). Those two bands can be assigned to the dipolar and quadrupolar components of the surface plasmon resonance (SPR) of the AgNPs. When the dimension of the particle approaches to the wavelength of the incident light, different part of the particle would experience different phase of the incident irradiation. As a result, higher multipolar modes, such as quadrupolar, octupolar, and even hexadecapolar modes can be excited.²⁵ In this case, the average size of the AgNPs was about 100 nm, resulting in coexistence of the dipolar and quadrupolar components in the extinct spectrum of the colloid. As the AgNPs were assembled on the glass slide modified with PVP, only a single sharp band was observed at 419 nm (red line). A similar spectral behavior of the immobilized AgNPs was reported by Malynych and Chumanov, who ascribed such a spectral phenomenon to the coherent Plasmon coupling resulting from the phase coherence for electron oscillations in neighboring particles, as the metal nanoparticles were assembled in a two-dimensional manner.²⁶ This coupled plasmon mode is dependent on size of the particles and the distance between the particles.²⁷ The adsorption of the PATP molecules on the surface of the AgNPs led to a shift of the SPR band to longer wavelength, mainly because of the change in dielectric constant of the media. Further assembly of the second layer of the silver nanoparticles resulted in a broad band with a maximum at 431 nm and an increase in intensity of the SPR band (blue line). The increase in the intensity of the SPR band reflects increase in the amount of the assembled particles. As indicated by the SEM images (Fig. 2B), during the second assembly, some of the AgNPs were assembled as the second particle layer, whereas the others were inserted into the first particle layer. Therefore, total amount of the AgNPs would be greatly increased. The shift and broadening of the SPR band, relative to those of the single layer assembly, could result from a more complicated coupling of the silver nanoparticles, which generate the Ag/PATP/Ag junctions, and are no long in the same plane.

The SERS spectra of the PATP molecules adsorbed on AgNPs single layer and in the Ag/PATP/Ag junctions were measured, and the results are shown in Fig. 2D. Both of the spectra are dominated by four strong bands at about 1078, 1143, 1390, and 1438 cm^{-1} , which can be assigned to ν_{7a} , ν_{9b} , ν_{3b} and ν_{19b} vibrations, respectively. Upon the assembly of the second layer of AgNPs, a considerable increase in the absolute intensity of the SERS spectrum and obvious changes in relative intensity were observed. For example, the additional enhancement factors for the bands at 1078 and 1143 cm^{-1} are 50 and 120 respectively. Two aspects are considered to be responsible for the great enhancement of the SERS signal of the interconnected PATP molecules: enhanced electromagnetic field in the molecular junction between the silver particles and chemical enhancement based on photoinduced charge transfer mechanism between the PATP molecules and metal particles. It has been well documented by a number of researches that a drastic enhancement of electromagnetic field occurs in the junctions or nanogaps between two metal particles due to plasmon coupling between the metal particles within a close distance.²⁸ Such an effect results in a huge intensification of the Raman scattering of molecules inside the junction. In this case, the interconnection of the PATP molecules between the two silver nanoparticles spontaneously generated a metal/molecules/metal junction. Therefore, the interconnected PATP molecules would experience the electromagnetic field greatly amplified by the plasmon coupling between two silver nanoparticles, leading to a great enhancement of the Raman scattering of the PATP molecules. On the other hand, as we demonstrated previously, charge transfer between the particles through the interconnecting molecules may also play a crucial role for the enhancement of Raman scattering of the interconnected PATP molecules.²⁹ Such an enhancement strongly depends on two factors: matching between the Fermi level of the metal with the HOMO and LUMO levels of the PATP molecules and dipolar momentum of the interconnecting molecules. Consequently, the b_2 modes at 1143, 1390, and 1438 cm^{-1} , which associated with the charge transfer between PATP molecules and metal, are specifically enhanced.

As aforementioned, the SERS behavior of the interconnected PATP molecules in the Ag/PATP/Ag junctions involves both EM mechanism and CT mechanism associated with the particular structure of the Ag/PATP/Ag junctions. It is expected that the electromagnetic field between the particles and/or the photoinduced charge transfer process could be largely associated with the nature of the particles. To elucidate this, we adopted surface modification of the silver nanoparticles with molecules to alter the microenvironment of the silver nanoparticles. The pristine Ag/PATP/Ag junctions were immersed in a solution containing molecules, such as n-octanethiol, 1,8-Octanedithiol, TP, 1,4-BDT, or 4-MPY, to allow the molecules to be adsorbed on the surface of the silver nanoparticles. Those molecules can only be adsorbed on the surface of the silver nanoparticles in the second layer. The silver nanoparticles in the first layer would maintain its original state, due to the surface of those particles was already occupied by the PATP molecules. Fig. 3 shows SERS spectra of the Ag/PATP/Ag junctions after modification of the adsorbed molecules. It should be pointed out that all the spectra were dominated with the signal from the interconnected PATP molecules. The signals from the modified molecules were relatively weak (for example, the inserted spectrum of TP), because the PATP molecules interconnected between two silver nanoparticles gained huge enhancement as aforementioned. From the spectra in Fig. 3, it was found that the modification of

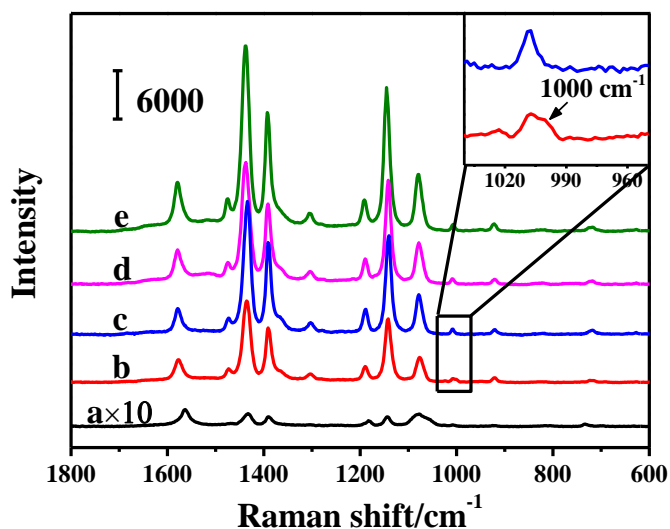


Fig.3 SERS spectra of Ag/PATP/Ag junctions modified with (a) 1, 4-BDT, (b) TP, (c) 1,8-octanedithiol, (d) n-octanethiol, (e) no molecule adsorption.

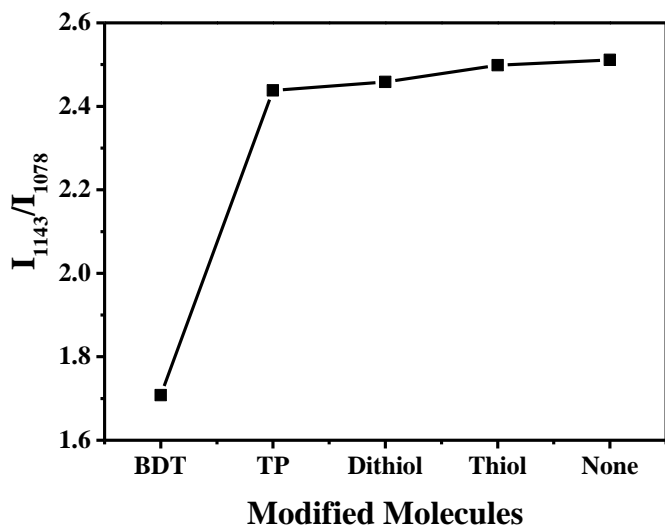


Fig.4 Variation of intensity ratio of the bands at 1143 and 1078 cm^{-1} of Ag/PATP/Ag junctions modified with different molecules.

n-octanethiol and 1,8-octanedithiol led to only a negligible spectral change for the Ag/PATP/Ag junctions. However, noticeable changes in the intensity of the SERS signals (Fig. 3a-d), relative to the original spectrum of the pristine Ag/PATP/Ag junctions, were observed as the junctions were modified with TP and 1,4-BDT modification. Moreover, a careful inspection of the SERS spectra indicates that the relative intensity of individual bands also varied as the assemblies were adsorbed with different molecules, as demonstrated in Fig. 4. For example, the relative intensity of the band at 1143 cm^{-1} (b_2 mode) to the band at 1078 cm^{-1} (a_1 mode), I_{1143}/I_{1078} , changed from 2.51 for the pristine Ag/PATP/Ag junctions to 1.71 for 1,4-BDT modified Ag/PATP/Ag junctions. The variation in absolute intensity of SERS spectra and relative intensities of individual bands for the Ag/PATP/Ag junctions modified with different molecules have

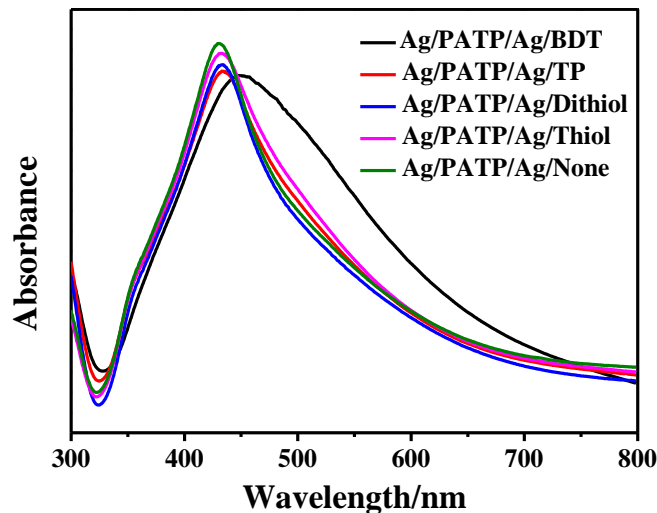


Fig.5 Extinction spectra of Ag/PATP/Ag junctions modified with different molecules: (a) 1,4-BDT, (b) TP, (c) dithiol (1,8-octanedithiol), (d) Thiol (n-octanethiol), (e) None (no molecule modified).

to be related to the influence of the adsorbed molecules on the SERS mechanisms arising from the particular structure of the junctions. Therefore, the effect of the adsorbed molecules on the EM and CT mechanisms for the SERS enhancement of the interconnected PATP molecules was discussed next.

Normally, the EM enhancement is always associated with the SPR band of the metallic nanoparticles or nanostructures.^{30, 31} We examined the influence of the adsorption of the molecules on the extinction spectrum of the Ag/PATP/Ag junctions. Fig. 5 shows the extinction spectra of the Ag/PATP/Ag assemblies after modification with different molecules. The SPR bands located at 430 nm for the pristine Ag/PATP/Ag junctions shifted to 432, 432, 434, 445 nm, as the junctions were adsorbed with n-octanethiol, 1,8-octanedithiol TP, and 1,4-BDT molecules, respectively, along with a slight decrease in the intensity of the band. The relatively large spectral alteration for 1,4-BDT is particularly noticed which is not associated with the absorption of 1,4-BDT itself as the absorption band of 1,4-BDT is located at 259 nm (Fig. S1, Supporting Information). Therefore, we believe that the large spectral change for 1,4-BDT could result from a strong interaction between the adsorbed 1,4-BDT and metal surface, which will be discussed later. In fact, the SPR band of the Ag/PATP/Ag junctions strongly depends on the surface coverage of the 1,4-BDT molecules. As demonstrated in Fig. S2, the SPR band located at 437 nm for the pristine Ag/PATP/Ag junctions gradually shifted to 448, 453, 457, 460 nm for the Ag/PATP/Ag junctions adsorbed with 1,4-BDT in a 1 mM 1,4-BDT solution for 10, 20, 40, or 60 min, respectively. That is, larger surface coverage of 1,4-BDT leads to a shift of SPR band of the Ag/PATP/Ag junctions to longer wavelength. Nevertheless, the SPR bands for all the assemblies were still far away from the 532 nm excitation used for the SERS measurements. It seems that under excitation of 530 nm, the adsorption of the molecules on the assemblies could only have little effect on the electromagnetic field arising from the coupling of the neighboring silver nanoparticles that are interconnected with the PATP molecules. As aforementioned, the electromagnetic coupling between the neighboring silver nanoparticles comes from the coherent plasmon coupling resulting from the phase coherent electron oscillations in

neighboring particles. Relatively uniform modification of the molecules on the surface of the silver nanoparticles may not have large effect on the coherent electron oscillations inside the nanoparticles.

Therefore, the CT mechanism could be the main factor responsible for the changes in SERS spectra of the assemblies modified with molecules. The CT mechanism for the metal/molecule/metal junction system involves the charge transfer between metal nanoparticles through the interconnecting molecules, which depends on the matching between the Fermi level of the metal with the HOMO and LUMO levels of the PATP molecules. The Fermi level of the metal is closely related to the local electronic density on the surface of the metal, where the PATP molecules were attached. In this case, the adsorption of the molecules on the silver nanoparticles in the second layer would disturb the electron distribution on the silver surface, due to the formation of surface chemical bonds and possible other interaction of the adsorbed molecules with the surface of the silver nanoparticles. Such an effect would be expected to depend on the type of the adsorbed molecules. As demonstrated in Fig. 3, the effect of the adsorbed *n*-octanethiol and 1,8-octanedithiol on the SERS signal of the PATP molecules in the Ag/PATP/Ag junctions was quite small, whereas a great variation in intensity of the SERS signal of the PATP molecules was observed as the junctions were modified with TP and 1,4-BDT. The fact that the formation of Ag-S bond of *n*-octanethiol and 1,8-octanedithiol with the silver metal only led to negligible alteration of the SERS signal of the interconnected PATP molecules may suggest that the dominant SERS enhancement factor is from the huge EM enhancement in the particular molecular junction. Slight variation from the formation of Ag-S bands might not be sufficient to influence overall SERS enhancement of the Ag/PATP/Ag junctions. On the other hand, the distinct spectral changes in the cases with TP and 1,4-BDT modifications indicate that there are additional interactions between the adsorbed molecules and the silver nanoparticles, that would largely reduce the contribution from the CT mechanism. The major difference in the molecular structures between *n*-octanethiol and 1,8-octanedithiol and TP, 1,4-BDT is that the latter possesses conjugated structure of benzene, which may result in additional interaction between the adsorbed molecules and metal surface and delocalization of the free electrons of the silver nanoparticles to the conjugated structure of the molecules. In fact, the TP molecules normally adopt a tilted orientation on the silver surface,³² whereas the 1,4-BDT molecules take a flat orientation with respect to the silver surface.³³ Therefore, a stronger interaction between surface of the AgNPs and benzene ring of the adsorbed molecules can be expected between the silver nanoparticles and the TP or 1,4-BDT molecules. As a result, the free electron in the silver nanoparticles could be more delocalized to the conjugated structures of the adsorbed TP and 1,4-BDT molecules. In particular, the intensity of the SERS signal of the Ag/PATP/Ag junctions decreases with increasing of the surface coverage of 1,4-BDT (Fig. S3), which is in parallel to the SPR results (Fig. S2). The delocalization of the free electrons in the silver nanoparticles would largely influence the Fermi level of the silver nanoparticles, which may result in less matching between the Fermi level of the metal with the HOMO and LUMO levels of the interconnected PATP molecules, thus, less CT contribution to the SERS signal of the Ag/PATP/Ag junctions. Such a large change in the CT contribution may be directly reflected by substantial weakening of the SERS spectral of the interconnected PATP molecules. According to the theory of the CT mechanism, Raman tensor elements are represented as

$\alpha = A + B + C$.³⁴ Term A represents a Franck–Condon contribution, and B and C terms represent Herzberg–Teller contributions, which correspond to molecule-to-metal and metal-to-molecule charge transfer transitions, respectively. In the case of the PATP molecules interacting with silver metal, only A and C terms are involved in the SERS enhancement. The nontotally symmetric vibrational modes (b_2 modes) can only be enhanced through the C term, whereas both A_K and C terms determine the enhancement of the totally symmetric vibrational modes (a_1 modes). The fact that both a_1 and b_2 modes of the interconnected PATP molecules were influenced by the adsorption of the TP and 1,4-BDT molecules indicates that both A and C terms were altered in Ag/PATP/Ag junctions in the presence of TP and 1,4-BDT molecules. Nevertheless, such an effect is dependent to the adsorbed molecules. Variation in different vibrational modes of the interconnected PATP molecules was still observed upon adsorption of TP and 1,4-BDT. For example, I_{1143}/I_{1078} of the

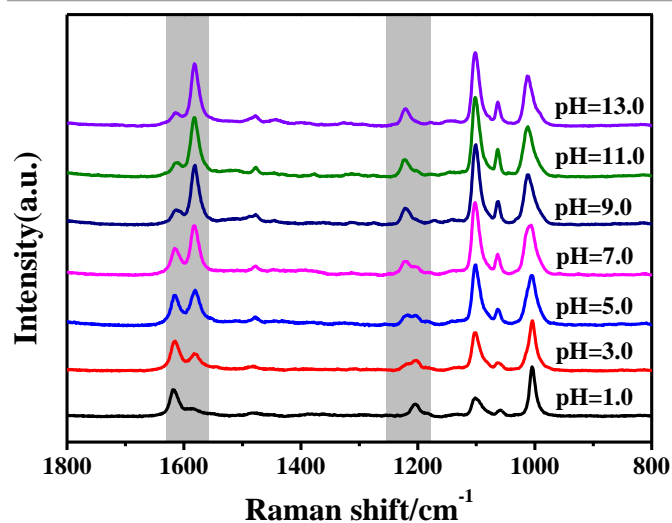


Fig. 6 pH-dependent SERS spectra of 4-MPY adsorbed on single layer of AgNPs.

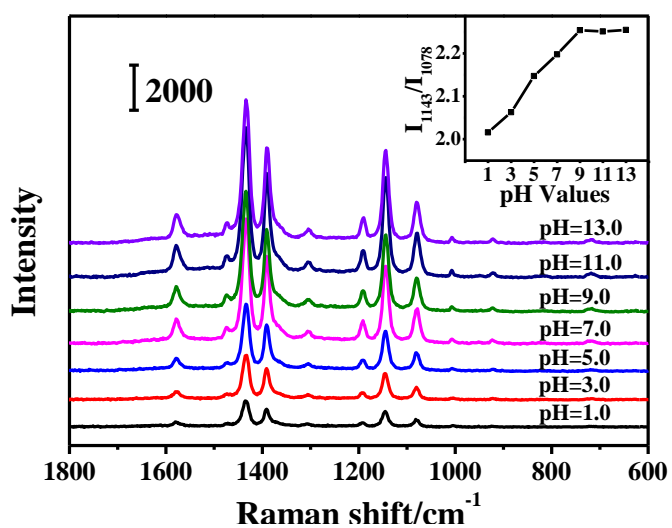


Fig. 7 pH-dependent SERS spectra of Ag/PATP/Ag junctions; Insert: variation of intensity ration of the bands at 1143 and 1078 cm^{-1} with pH values.

interconnected PATP molecules changed from 2.52 for TP adsorption to 1.71 for 1,4-BDT adsorption.

To further verify the effect of the delocalization of free electrons of the silver nanoparticles on the SERS behavior of the interconnected PATP molecules, the SERS spectra of 4-MPY molecules adsorbed on the single layer of silver nanoparticles and the junction assemblies were measured in the solutions with different pH values. Because the pyridine of the adsorbed 4-MPY can exist either in protonated form or deprotonated form, depending on the pH value of the media, the combination of proton with the nitrogen in the pyridine of the adsorbed 4-MPY molecules by sharing the lone pair of electrons at nitrogen atom would influence the charge distribution in the conjugated pyridine ring structure, and in turn the delocalization of the free electrons in silver nanoparticles to the pyridine ring. The protonation/deprotonation process of the adsorbed 4-MPY can be clearly seen in a series SERS spectra of MPY adsorbed on the silver nanoparticles assembled in single layer, as shown in Fig. 6. Two pairs of bands, 1200/1220 cm^{-1} and 1580/1614 cm^{-1} (shaded area) are quite sensitive to the pH value of the solutions.^{35,36} The intensities of the bands at 1200 and 1614 cm^{-1} for the N-protonated form of 4-MPY molecules decreased with decreasing of the pH value, whereas the intensities of the bands at 1220 and 1580 cm^{-1} for the N-deprotonated form correspondingly increased. In the case of the Ag/PATP/Ag junctions adsorbed with MPY molecules, a similar tendency in variation of the intensity of the SERS spectra of the PATP molecules in the Ag/PATP/Ag junctions was observed, as shown in Fig. 7. The absolute intensity of the SERS spectra of the interconnected PATP molecules increased with increasing of the pH value of the media (Insert in Fig. 7). This phenomenon can be interpreted based on the fact that sharing the lone pair of electrons at the nitrogen atom in pyridine with the proton would lead to the free electrons in silver nanoparticles to be more delocalized to the conjugated pyridine ring. In parallel to the case of the TP and 1,4-BDT modification, delocalization of the free electrons in the silver nanoparticles results in less CT contribution to the SERS enhancement of the interconnected PATP molecules. However, it should be pointed out that to gain a full insight into this phenomenon, a theoretic calculation should be conducted.^{37,38}

Conclusions

In summary, we constructed the Ag/PATP/Ag molecular junctions through a layer-by-layer assembly to investigate the influence of the adsorption of molecules on the SERS behavior of the interconnected PATP molecules. It has been demonstrated that the molecules with conjugated structure showed large effect on the SERS enhancement of the PATP molecules. Only slight effect on the huge electromagnetic field arising from the coupling between neighboring silver nanoparticles was observed upon the modification of the adsorbed molecules. However, the strong interaction between silver nanoparticles and adsorbed molecules could lead to large alteration in the CT contribution to the SERS enhancement of the PATP molecules, depending on the structure of the adsorbed molecules. The weakening of the CT contribution, in the case of aromatic thiols, is ascribed to the delocalization of the free electrons in the silver nanoparticles to the conjugated structure of the modified molecules. The results may be helpful for comprehensive understanding the SERS phenomena of the molecules in the gap between metals and for the design of advance structures based on molecule-metal nanoparticle assembly. It should be pointed out that to gain further insight into the effect of the modification of molecules on

metal/molecule/metal junction, a precise design of molecular structures is necessary.

Acknowledgements

Financial supports from the Nature Science Foundation of China (Nos.21336005), Ministry of Science and Technology of China (Nos. 2014EG111224), and Project of Scientific and Technologic Infrastructure of Suzhou (Nos. SZS201207) are gratefully acknowledged.

Notes and references

^aCollege of Chemistry, Chemical Engineering and Materials Science, and Key Lab of Health Chemistry and Molecular Diagnosis of Suzhou, Soochow University, Suzhou 215123, P. R. China, zhq@suda.edu.cn;

^bCollege of Physics, Optoelectronics and Energy, Soochow University, Suzhou 215006, P. R. China. jwzheng@suda.edu.cn.

Electronic Supplementary Information (ESI) available: [details of any supplementary information available should be included here]. See DOI:10.1039/b000000x/

- 1 A. Zabet-Khosousi and A. A. Dhirani, *Chem Rev*, 2008, **108**, 4072-4124.
- 2 J. Liao, S. Blok, S. J. van der Molen, S. Diefenbach, A. W. Holleitner, C. Schonenberger, A. Vladyka and M. Calame, *Chem Soc Rev*, 2015, **44**, 999-1014.
- 3 M. A. Mangold, M. Calame, M. Mayor and A. W. Holleitner, *J Am Chem Soc*, 2011, **133**, 12185-12191.
- 4 Z. Y. Li, S. Butun and K. Aydin, *Acs Photonics*, 2014, **1**, 228-234.
- 5 Y. Yin, T. Qiu, J. Q. Li and P. K. Chu, *Nano Energy*, 2012, **1**, 25-41.
- 6 T. A. Gschneidner, Y. A. D. Fernandez and K. Moth-Poulsen, *J Mater Chem C*, 2013, **1**, 7127-7133.
- 7 M. Hu, F. S. Ou, W. Wu, I. Naumov, X. M. Li, A. M. Bratkovsky, R. S. Williams and Z. Y. Li, *J Am Chem Soc*, 2010, **132**, 12820-12822.
- 8 A. B. Zrimsek, A. I. Henry and R. P. Van Duyne, *J Phys Chem Lett*, 2013, **4**, 3206-3210.
- 9 H. Haick, J. Ghabboun, O. Niitsoo, H. Cohen, D. Cahen, A. Vilan, J. Y. Hwang, A. Wan, F. Amy and A. Kahn, *J Phys Chem B*, 2005, **109**, 9622-9630.
- 10 D. Conklin, S. Nanayakkara, T. H. Park, M. F. Lagadec, J. T. Stecher, X. Chen, M. J. Therien and D. A. Bonnell, *Acs Nano*, 2013, **7**, 4479-4486.
- 11 E. Leary, A. La Rosa, M. T. Gonzalez, G. Rubio-Bollinger, N. Agrait and N. Martin, *Chem Soc Rev*, 2015, **44**, 920-942.
- 12 P. Z. El-Khoury, D. H. Hu and W. P. Hess, *J Phys Chem Lett*, 2013, **4**, 3435-3439.
- 13 X. Gong, Y. Bao, C. Qiu and C. Y. Jiang, *Chem Commun*, 2012, **48**, 7003-7018.
- 14 M. M. Harper, K. S. McKeating and K. Faulds, *Phys Chem Chem Phys*, 2013, **15**, 5312-5328.
- 15 J. F. Li, Y. F. Huang, Y. Ding, Z. L. Yang, S. B. Li, X. S. Zhou, F. R. Fan, W. Zhang, Z. Y. Zhou, D. Y. Wu, B. Ren, Z. L. Wang and Z. Q. Tian, *Nature*, 2010, **464**, 392-395.
- 16 N. Zohar, L. Chuntunov and G. Haran, *J Photoch Photobio C*, 2014, **21**, 26-39.
- 17 J. Theiss, P. Pavaskar, P. M. Echternach, R. E. Muller and S. B. Cronin, *Nano Lett*, 2010, **10**, 2749-2754.

- 18 R. W. Taylor, T. C. Lee, O. A. Scherman, R. Esteban, J. Aizpurua, F. M. Huang, J. J. Baumberg and S. Mahajan, *Acs Nano*, 2011, **5**, 3878-3887.
- 19 X. M. Zhao and M. D. Chen, *Rsc Adv*, 2014, **4**, 63596-63602.
- 20 M. R. Gartia, T. C. Bond and G. L. Liu, *J Phys Chem A*, 2011, **115**, 318-328.
- 21 L. L. Zhao, L. Jensen and G. C. Schatz, *Nano Lett*, 2006, **6**, 1229-1234.
- 22 D. R. Ward, N. K. Grady, C. S. Levin, N. J. Halas, Y. P. Wu, P. Nordlander and D. Natelson, *Nano Lett*, 2007, **7**, 1396-1400.
- 23 E. C. Le Ru, J. Grand, I. Sow, W. R. C. Somerville, P. G. Etchegoin, M. Treguer-Delapierre, G. Charron, N. Felidj, G. Levi and J. Aubard, *Nano Lett*, 2011, **11**, 5013-5019.
- 24 D. D. Evanoff and G. Chumanov, *J Phys Chem B*, 2004, **108**, 13948-13956.
- 25 K. L. Kelly, E. Coronado, L. L. Zhao and G. C. Schatz, *J Phys Chem B*, 2003, **107**, 668-677.
- 26 S. Malynych and G. Chumanov, *J Am Chem Soc*, 2003, **125**, 2896-2898.
- 27 M. K. Kinnan and G. Chumanov, *J Phys Chem C*, 2010, **114**, 7496-7501.
- 28 H. X. Xu, J. Aizpurua, M. Kall and P. Apell, *Phys Rev E*, 2000, **62**, 4318-4324.
- 29 Q. Zhou, X. Li, Q. Fan, X. Zhang and J. Zheng, *Angew Chem Int Edit*, 2006, **45**, 3970-3973.
- 30 M. Moskovits, *Rev Mod Phys*, 1985, **57**, 783-826.
- 31 A. Campion and P. Kambhampati, *ChemSoc Rev*, 1998, **27**, 241-250.
- 32 K. T. Carron and L. G. Hurley, *J Phys Chem-Us*, 1991, **95**, 9979-9984.
- 33 S. W. Joo, S. W. Han and K. Kim, *J Colloid Interf Sci*, 2001, **240**, 391-399.
- 34 J. R. Lombardi, R. L. Birke, T. H. Lu and J. Xu, *J Chem Phys*, 1986, **84**, 4174-4180.
- 35 J. W. Hu, B. Zhao, W. Q. Xu, B. F. Li and Y. G. Fan, *Spectrochim Acta A*, 2002, **58**, 2827-2834.
- 36 Y. Chao, Q. Zhou, Y. Li, Y. Yan, Y. Wu and J. Zheng, *J Phys Chem C*, 2007, **111**, 16990-16995.
- 37 F. Mirjani, J. M. Thijssen and M.A. Ratner, *J. Phys. Chem. C* 2012, **116**, 23120-23129.
- 38 M. Banik, V. A. Apkarian, T.-H. Park and M. Galperin, *J. Phys. Chem. Lett.* 2013, **4**, 88-92.